Gold neutron-capture cross section from 3 to 550 keV*

R. L. Macklin and J. Halperin
Oak Ridge National Laboratory, Oak Ridge, Tennessee 37830

R. R. Winters
Denison University, Granville, Ohio 43023

(Received 24 June 1974)

A careful remeasurement of the ^{197}Au(n,γ) cross section using the pulse height weighting technique in small scintillators has been completed. The 4.9 eV resonance was used for calibration and the ^{6}Li(n,α) cross section for flux shape. Estimated errors range from 1.4% near 30 keV to 3.3% at 550 keV. Individual resonance parameters were deduced in the 2.6–4.9 keV range and the fluctuations over 10's of resonances were analyzed below 90 keV. The fluctuations are larger than expected, limiting the precision attainable with monoenergetic sources using this standard. The fluctuation intensity appears to indicate intermediate resonance structure in the compound nucleus with ~10 keV width and ~40 keV spacing.

[NUCLEAR REACTIONS ^{197}Au(n,γ), $E=3$–550 keV; measured $\sigma(E)$; deduced ^{198}Au level parameters, strength functions, spacings.]

I. INTRODUCTION

Gold, largely because of its convenient neutron induced radioactivity, chemical and isotopic purity, large thermal neutron capture, and resonance capture integral has become the principal standard in relative neutron-capture measurements. In the tens to hundreds of keV energy range it has also been used as a standard for cross section measurements relevant to stellar nucleosynthesis and fission reactor design. With increasing emphasis on precisions of 1–2% the fluctuations in this standard cross section can no longer be ignored and we find that it is not simple to predict their size from theory. The average over many compound nucleus resonances is found to be remarkably well fitted up to 150 keV by energy independent strength functions consistent with the statistics of the isolated resonances seen below 5 keV. (At higher energies, competition with inelastic scattering becomes increasingly important.) The fluctuations about the average, however, show substantial structure only qualitatively understood as intermediate (hallway) states between the optical model "doorway" states and the relatively long-lived compound nucleus states.

II. EXPERIMENT

The neutron-capture rate in the present experiment is measured by detecting the prompt ($<5\times10^{-9}$ sec) capture γ rays from the compound nucleus' deexcitation. A symmetrically placed pair of scintillation detectors are used to reduce the effect of possible shifts in sample or neutron beam alignment to less than 0.2%. Independence of the primary yield data from changes in the capture cascade spectrum is achieved by pulse height weighting for pulses above a sharp 153 keV bias. This independence is confirmed to ±1% for neutron-capture spectra as diverse as those from Ho, Au, and ^{238}U (see Discussion); still greater independence is inherent for this experiment in the use of the 4.9 eV saturated gold resonance to measure the efficiency of the detectors. (Calibrated radioactive sources have also been used to check that the detector and monitor efficiencies and geometry factors are within a few percent of the values calculated from composition, γ ray cross sections, etc.)

The neutron time-of-flight facility and apparatus (flight path 7, 40 m station) have been described in some detail in earlier publications.[1]

While gold capture yields have been checked for several years, the present results are based on a two-week cycle of four runs interspersed with 4.9 eV saturated resonance efficiency calibrations, primarily to check on and average over possible small uncontrolled drifts in detector and electronic amplifier gains. Such drifts observed at other times have been as high as 2% in a week. As there was no evidence of drift (within counting statistics), the calibrations and the runs have each been averaged, and the effective cross sections per atom computed.

Our data rates are roughly one event each five neutron pulses so we can set the time interval digitizer (clock) to operate no more than once per pulse. The counting system is again restarted at the next neutron burst. This makes the clock dead time

dominant and the average correction (0 to 20% typically) is readily computed. The sum $S(t)$ of all counts recorded at shorter flight times than t compared to the number of neutron pulses P in the run determines the fraction of the run when the clock was dead at time t and the correction factor is just $1/[1-S(t)/P]$.

The accelerator independent backgrounds are sampled during each run near 900 μsec flight time (11 eV) where the ^{10}B overlap filter is nearly black to neutrons, as well as in side experiments with the beam stop inserted in the flight path or when the accelerator is not running. A small neutron background is seen in runs with no sample; the net effect is scaled to source intensity and subtracted from sample runs.

Our sample scattered neutron sensitivity has been measured by several techniques, the most comprehensive using the off resonance scattering from ^{208}Pb and C samples [see Fig. 3 of Ref. 1(a)]. The ^{208}Pb scattering data have been parametrized in terms of a $1/v$ component and resonance capture in the fluorine and aluminum of the detector and housing. The resonance effects are shifted and smeared to match the elastic scattering energy loss of lighter targets. Thus the scattered neutron sensitivity (typically a few times 10^{-4}) can be calculated for any sample at any energy in our range (2.5–1100 keV). Where well isolated resonances are seen (2.6–4 keV), peak to valley ratios of 50 were noted in the raw data before any corrections were applied.

The energy dependence of the neutron flux was monitored by a 0.05 cm ^{6}Li glass scintillator in transmission.[2] The perturbations introduced by the glass have been described previously.[1] The ^{6}Li(n, α) cross section parametrization used is given in Appendix I and discussed later.

III. RESONANCE ANALYSIS

Our neutron energy resolution below 90 keV is dominated by the neutron moderation time and is a little better than 0.2% full width at half-maximum. This allows isolated resonance parameter extraction below 5 keV or so, primarily for s-

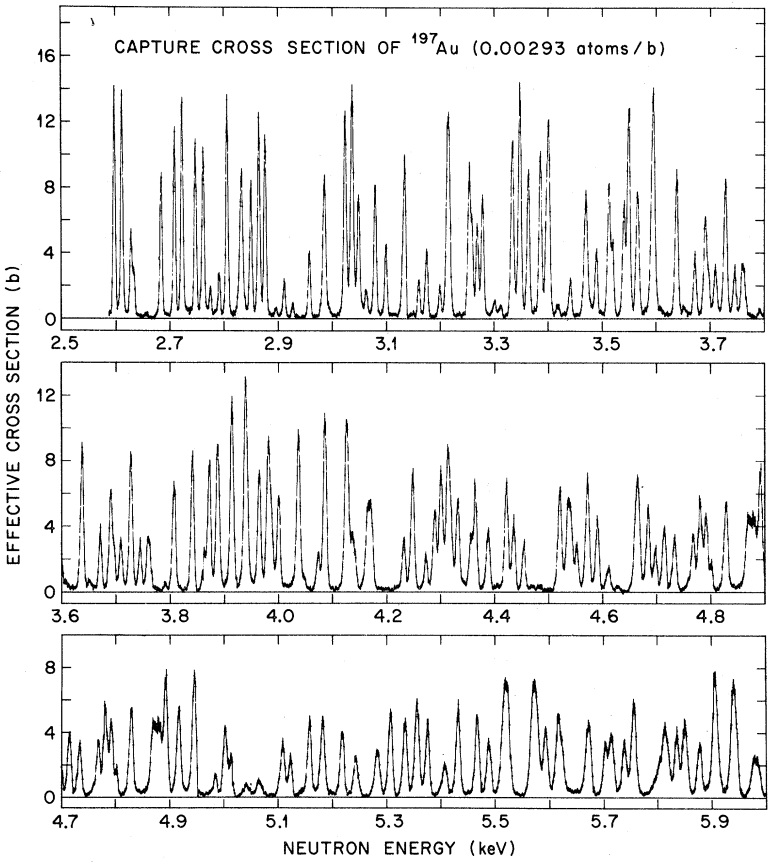

FIG. 1. Resonance structure in the ^{197}Au(n, γ) effective cross section for a 0.002 93 atom/b sample. Most of the peaks correspond to isolated compound nuclear levels formed by s-wave neutrons.

TABLE I. Isolated resonance parameters for $^{197}Au(n,\gamma)$ derived from the capture cross section, 2597–4827 eV.

E_n [a] (eV)	$g\frac{\Gamma_\gamma\Gamma_n}{\Gamma}$ (meV)	S.D. [b]	E_n [a] (eV)	$g\frac{\Gamma_\gamma\Gamma_n}{\Gamma}$ (meV)	S.D. [b]	E_n [a] (eV)	$g\frac{\Gamma_\gamma\Gamma_n}{\Gamma}$ (meV)	S.D. [b]	E_n [a] (eV)	$g\frac{\Gamma_\gamma\Gamma_n}{\Gamma}$ (meV)	S.D. [b]
2597	47.5	3.0	3160	10.3	1.0	3695	3.5	1.2	4289	47.6	2.7
2611	47.9	3.0	3174	20.7	1.5	3709	13.9	1.2	4300	64.8	3.5
2629	24.6	2.3	3199	6.2	0.6	3727	59.6	2.8	4315	57.2	4.8
2634	2.3	1.0	3214	89.7	4.0	3744	17.0	1.1	4332	39.2	2.2
2654	0.8	0.4	3255	43.1	8.0	3759	14.8	3.0	4356	29.4	2.1
2684	30.7	1.7	3258	22.0	6.6	3762	12.1	2.7	4364	48.1	2.6
2708	38.2	2.4	3267	24.0	1.7	3791	1.9	0.5	4388	33.9	1.8
2722	49.1	2.9	3277	37.5	2.4	3807	49.3	2.5	4422	60.9	2.9
2747	37.1	2.0	3300	4.3	0.9	3841	62.7	3.3	4435	33.6	1.8
2761	39.4	2.2	3311	2.8	0.7	3863	14.8	1.4	4454	21.1	1.3
2774	4.6	0.6	3333	65.1	3.7	3872	58.6	3.2	4521	60.5	3.2
2790	7.2	0.8	3347	87.3	4.5	3888	74.4	3.9	4537	35.8	6.3
2805	47.5	2.4	3363	45.9	2.8	3914	90.0	4.1	4540	35.0	6.1
2832	55.0	3.5	3385	53.1	3.1	3939	95.7	4.3	4550	18.6	1.7
2849	33.2	2.3	3399	81.8	4.5	3964	53.0	2.8	4572	61.7	3.2
2864	48.7	3.0	3417	2.6	0.4	3982	92.3	7.4	4590	34.7	2.1
2876	44.9	2.8	3440	10.5	0.6	3986	9.8	3.0	4611	17.0	1.3
2896	1.4	0.2	3469	61.1	4.3	4000	40.3	2.3	4628	6.5	0.7
2911	9.0	0.6	3488	18.9	2.1	4036	76.7	3.4	4664	86.4	4.2
2926	2.5	0.2	3513	46.4	5.9	4046	3.6	0.7	4684	40.3	2.3
2957	16.2	0.9	3518	12.7	3.8	4072	11.8	0.9	4697	18.2	1.5
2985	49.1	2.5	3540	35.3	2.0	4086	88.3	3.8	4714	42.5	2.6
3024	61.3	3.2	3549	84.9	4.1	4126	103.3	5.0	4733	24.7	1.2
3036	81.7	4.1	3565	50.8	2.7	4137	32.6	2.3	4767	31.9	2.6
3048	33.0	2.1	3594	116.7	5.3	4165	37.6	6.9	4779	53.9	3.5
3062	4.5	0.8	3637	60.8	2.9	4170	46.7	7.3	4790	45.8	3.0
3079	37.3	2.3	3651	2.6	0.5	4232	21.5	1.3	4799	10.7	1.5
3099	16.4	0.8	3671	20.5	1.3	4248	61.2	3.0	4827	54.2	2.8
3132	49.2	4.6	3691	41.3	2.6	4272	15.3	1.1			

[a] Error estimates for resonance energies are 0.06%.
[b] The standard deviations include both systematic and statistical errors.

wave resonances. The effective cross sections are shown in Fig. 1. An automatic peak finding and Gaussian fitting computer code was used for preliminary resonance analysis as the experimental resolution is approximately Gaussian and much broader than the average neutron width. The areas found were corrected for resonance self-protection (a 2–19% effect for our 0.002 93 atom/b foil) and interpreted in terms of neutron and radiative widths (see Table I). Scattering data[3] for many of the resonances were combined with our capture data to derive values of $g\Gamma_n$ and $g\Gamma_\gamma$. For weaker resonances, where scattering data were not available, the average radiative width (0.120 eV) has been assumed in deriving $g\Gamma_n$.

The reported scattering data[3] gave a very low strength function (0.55×10^{-4}) in our energy range and disagreed similarly with 20 resonances between 1000 and 2150 eV for which a total width and spin had been determined.[15] We have therefore renormalized the scattering data to agree with the average for the 20 resonances cited. Perhaps not surprisingly the strength function deduced in our 2597–4827 eV energy range becomes $(2.0\pm0.1)\times10^{-4}$ (the indicated error is statistical only) in agreement with the value $(2.0\pm0.2)\times10^{-4}$ deduced from the transmission data[15] for all resonances below 2150 eV. More significantly the few reported values of $g\Gamma_n$ near 2600 eV agree well with those we deduce from our data in combination with the renormalized scattering data. The standard deviations listed include our propagated counting statistics and estimated systematic errors discussed later. Uncertainty in the spin values leads to less than ±1.5% error even for the strongest resonances.

Figure 2 shows the distribution of the analyzed resonances, leading to an average spacing of 19.4 ±2.0 eV (2.6–4.9 keV range). While there are a couple of additional tiny peaks discernable in Fig. 1 but deemed too small to analyze, there may also be a couple of exceptionally strong p-wave resonances included among those analyzed. Thus, the observed spacing may be taken as approximating

the s-wave resonance spacing for this energy range. It is consistent with the spacing found from fluctuation analysis (see later) for the 3–5 keV range; 26 ±9 eV. The increasing departure of the cumulative spacing from a linear relationship (see Fig. 2) is traditionally attributed to undetected small resonances. This situation is not favored here as the sensitivity of the capture measurement in s-wave reduced neutron width is about $2g\Gamma_n^0$ =0.04 meV. Only three widths smaller than this are reported at any energy. One expects 92% of the resonances to exceed this limit from the Porter-Thomas distribution. Thus we feel that a change of 40% or so in average spacing over the range 0–5 keV is probably real (see later discussion).

IV. AVERAGE NEUTRON-CAPTURE CROSS SECTION

In the region above a few keV neutron energy, individual resonances cannot be resolved but the average cross section can be well described by strength functions, at least below the threshold for competition from inelastic scattering.[4] In the present case this procedure has produced satisfactory fits to the data up to 150 keV (see Fig. 3) although a first inelastic threshold is expected at 78 keV. Only the data below 90 keV were used in fitting to the four strength functions, S^0, S^1, S^2, and $\Gamma\gamma/D^0$ to avoid possible distortion by the inelastic competition. The fitting procedure involves the assumption of conventional angular momentum barriers, the Porter-Thomas neutron width distribution (for $l=0$), and a $(2J+1)$ level density dependence.[1] The fit is an attempt to best represent the local average cross section by weighting for equal percentage deviation from the fit at each energy.

The same formalism also allows us to calculate and correct for the average resonance self-protection and multiple scattering in the 0.05 cm sample we used.[5] The former effect shrinks steadily with energy, leaving the latter dominant at high energy, peaking at 4.8% near 100 keV. The two (average) effects were calculated to cancel near 5 keV, where of course most individual resonances can still be resolved.

The other correction applied to the data in Fig. 3 is for direct detection of inelastic γ rays along with the capture cascade which sets in significantly above 240 keV and rises to 15% near 560 keV using reported inelastic γ ray yields.[6-8] Another procedure leading to this correction is to use only our higher bias data, but it would involve the uncertainty of a longer extrapolation (from say 450 keV pulse height rather than 153 keV) to zero for the capture cascade. As the 4.9 eV saturated resonance we used for primary normalization of our efficiency ratio is thought to involve an atypically hard cascade we preferred the former method in the case of gold.

The neutrons inelastically scattered (rather than elastically) have an increased chance of absorption in the foil as recently emphasized by Devaney.[10] (See Appendix II.) This enhancement gives an additional correction not exceeding 0.3% and is most conveniently incorporated with the multiple

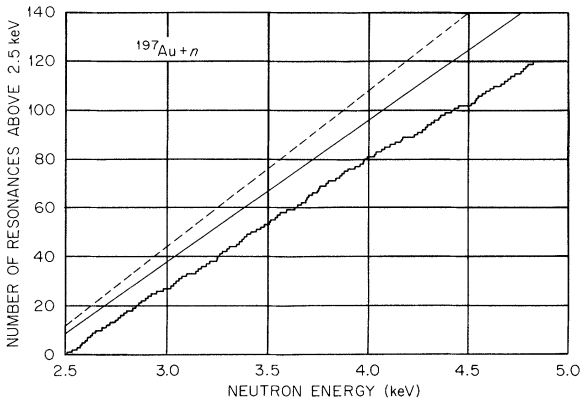

FIG. 2. Cumulative distribution of the observed resonances above 2500 eV. The first four are from a transmission measurement (Ref. 15). The solid straight line is from the same reference and the dashed line from a scattering cross section measurement (Ref. 3). These lines represent the cumulative distributions of resonance spacing at lower energies.

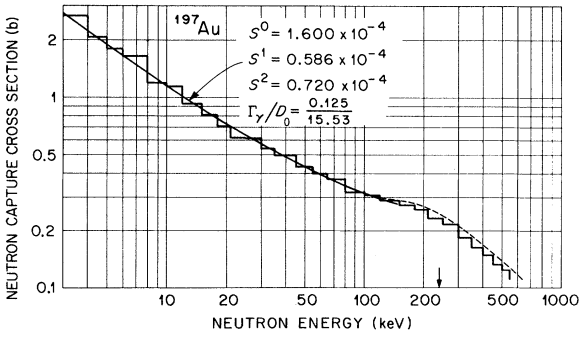

FIG. 3. Histogram of the ^{197}Au(n, γ) cross section. The sample yields have been corrected for average resonance self-protection, multiple scattering, and γ ray self-absorption. A correction for inelastic scattering has been applied at energies above the threshold indicated by the arrow. The dotted curve (coincident with the solid line s-, p-, d-wave strength function fit from 23 to 120 keV) is from an evaluation of earlier measurements by Poenitz (Ref. 20). Recent data from Le Rigoleur *et al.* (Ref. 21) above 70 keV agree well with ours.

elastic scattering correction considered previously.

From the strength functions and the additional assumption of a nearly constant radiative width one can calculate probability distributions of cross sections averaged over regions of interest. For instance, averaging over the range 23–25 keV gives an approximately normal distribution with a standard deviation of 4%. Thus, the actual deviations from the smooth strength function curve must also be measured with good resolution to permit accurate comparison with other measurements.

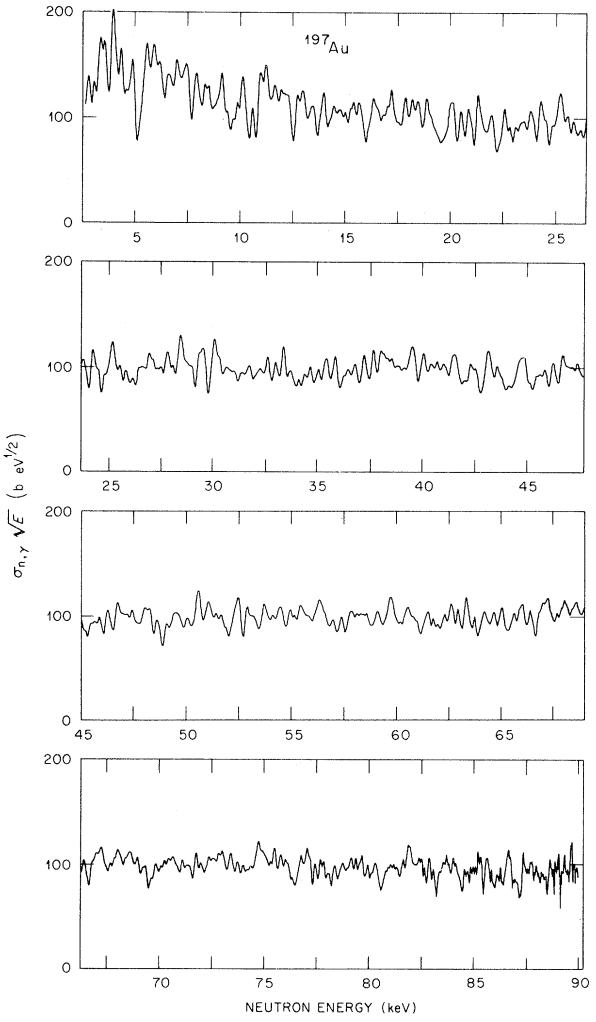

FIG. 4. Gold capture data smeared to a constant Gaussian resolution (175 eV full width at half-maximum) to average over tens of compound nucleus resonances. The fluctuations remaining can be analyzed for evidence of intermediate structure. Likewise, the departure of the cross section from smooth behavior over energy bands less than a few keV wide (as used in other earlier measurements of the cross section) can be evaluated.

As our resolution function for this experiment is approximately Gaussian with a full width at half-maximum (FWHM) of 175 eV near 90 keV, it is convenient to convolute our data at lower energies with a computed Gaussian of a width selected to give a constant 175 eV width. This is

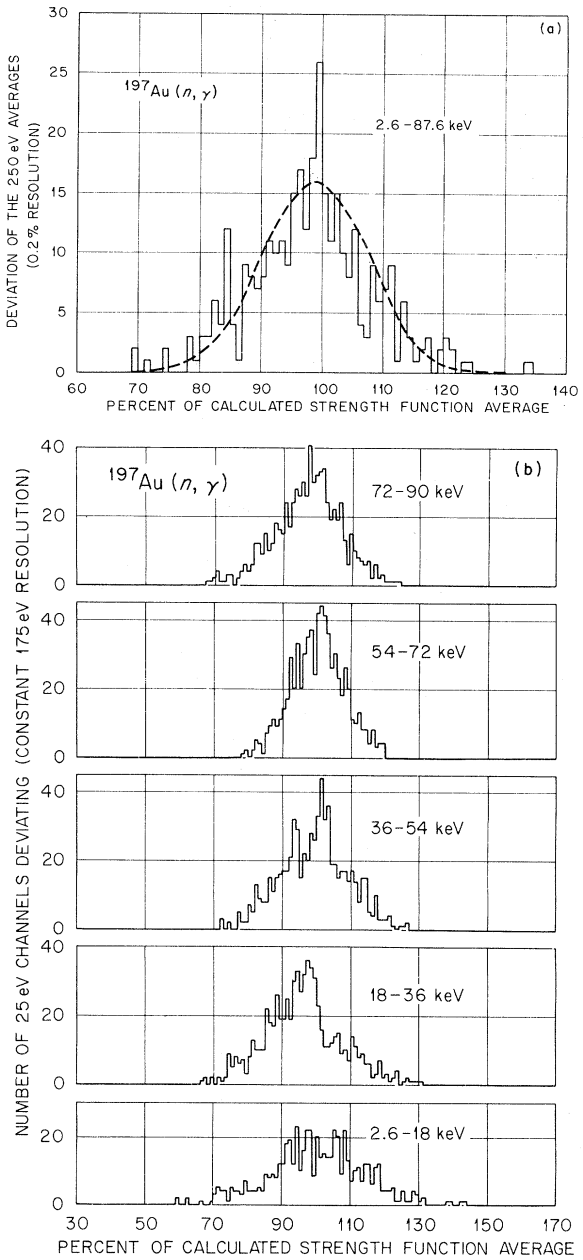

FIG. 5. (a) Au(n, γ) cross section fluctuations for 250 eV intervals. Deviations from the fit of Fig. 1 are plotted in 1% intervals. The dashed curve is a Gaussian such as is expected for uncorrelated data. (b) Au(n, γ) cross section fluctuation histograms for a constant 175 eV (FWHM) Gaussian resolution and 25 eV intervals.

conveniently many times the average s-wave level spacing so that individual levels do not dominate the deviations. These smoothed data are plotted in Fig. 4. Figure 5(a) shows the distribution of deviations for the combined data and Fig. 5(b), for five smaller, roughly equal energy intervals. The 100% corresponds to a nonlinear least squares adjusted four strength function fit[9] over the full 2.6–89 keV energy range.

A distribution free runs test[11] about the strength function fit for additional correlated structure shows possible correlation for 250, 500, and 750 eV intervals, just significant at the 95% probability level. As our resolution function introduces some such correlation, this is still not to be considered significant. For 1000 eV intervals the number of runs is within one standard deviation of the expected value.

In an earlier paper[12] Egelstaff has applied the statistical behavior of neutron cross sections to fluctuation analysis for several restricted cases, He showed that the level spacing parameter D_0 (the spacing for $l=0$ levels) in particular is directly proportional to the variance of the cross section averaged over many resonances. In particular an interval (W) of $10D_0$ was found ample to produce less than 1% error in the analysis. In the intervening years evidence for the Porter-Thomas distribution of reduced neutron widths and the Wigner distribution of spacings (which enter the fluctuation equation) has accumulated, so the analysis for spacing parameter can be applied with more confidence.

For the 2.6-90 keV neutron-capture cross sections of the present analysis, the fluctuations depend on the distribution laws of four widths Γ_n^0, Γ_n^1, Γ_n^2, Γ_γ, and the spacing D_0 in varying proportions. At low energy ($\Gamma_n \ll \Gamma$) Egelstaff's Eq. (3) applies

$$\frac{\mathrm{Var}(\sigma)}{\sigma^2} = \frac{D_0}{W}\left[\frac{\mathrm{Var}(\Gamma_n^0)}{(\Gamma_n^0)^2} + \frac{\mathrm{Var}(D_0)}{(D_0)^2}\right]. \qquad (1)$$

The first term in the bracket is 2.0 for the Porter-Thomas distribution (more generally $2/\nu$ for ν degrees of freedom in a χ^2 distribution). The second term is given[12] as 0.27 for the Wigner distribution.

Extending the formulation to the higher energies we obtain

$$\frac{\mathrm{Var}(\sigma)}{\sigma^2} = \frac{D_0}{W}\left[C_0^2\frac{\mathrm{Var}(\Gamma_n^0)}{(\Gamma_n^0)^2} + C_1^2\frac{\mathrm{Var}(\Gamma_n^1)}{(\Gamma_n^1)^2} + C_2^2\frac{\mathrm{Var}(\Gamma_n^2)}{(\Gamma_n^2)^2} + C_\gamma^2\frac{\mathrm{Var}(\Gamma_\gamma)}{\Gamma_\gamma^2} + \frac{\mathrm{Var}(D_0)}{(D_0)^2}\right] \qquad (2)$$

using as a basis the same simplifications [such as $(2J+1)$ spin dependence of the level density] employed in the four strength functions fitted to the average cross section.

The coefficients indicated (C_i or C_γ) refer to the relative effect of each parameter on the cross section and are functions of the energy. Indeed they are just the partial logarithmic derivatives of the average capture cross section. The C_2 coefficient is so small below 90 keV that the d-wave fluctuation term has been neglected. In the p-wave term we note that the states with spin $J=1$ and 2 can be formed with two channel spins each and we take this to imply two degrees of freedom in the appropriate χ^2 distribution. To facilitate the computation the p-wave term has been split among the four accessible spins and the coefficient calculated separately for each. The small relative variance of the distribution of radiative widths has been calculated for a χ^2 distribution of 197 degrees of freedom.[13]

To correspond to our resolution near 90 keV (< 175 eV FWHM Gaussian) the width W is taken as that of a rectangular function of equal variance, of $2\sqrt{3}$ times the standard deviation of the Gaussian.

Using the strength functions of Fig. 3, a 250 eV block size, and a single average radiative width of 0.125 eV ($D_0=15.53$), the predicted relative variance falls from 0.33 at 2.6 keV to 0.21 at 12.6 keV and changes little at the higher energies. It is immediately obvious from the amplitude excursions in Fig. 4 that this simple dependence is not what we find. (The frequency changes on the other hand correspond well to the two spin states for s-wave below 12 keV, shading into the more rapid p-wave dominance to 70 or 80 keV and finally the rapid flutter of the weak d-wave contribution.) The level spacing computed from the variance (subtracting the small variance of the counting statistics[12]) varies over a factor of 6, although the average over the whole energy range is 11.2 eV.

The change in the spacing parameter with energy would seem to call for some elaboration of the simplified theoretical parametrization we have employed. The first expectation might be for a different spacing for levels of opposite parity ($l=0$ and $l=1$). This idea would lead to a monotonic change with the energy of the spacing parameter found from fluctuation intensity. As we find more structure as a function of energy, this elaboration would clearly not be adequate by itself.

As the runs test for correlation from 2.6–90

keV falls well below the 95% probability level for intervals in excess of 750 eV, we may tentatively adopt the conclusion that the energy independent four strength function fit is adequate over a tenth of an MeV or so near 6.5 MeV excitation in ^{198}Au. A single particle model (such as those used to explain the peaks in neutron strength functions as a function of mass number) with the strength functions determined by levels a few MeV wide might be compatible with this approach. The variation of spacing parameter over a few tens of kilovolts might then be viewed as a manifestation of the spacing and width of the next most complicated class of levels. The compound nucleus levels would then be viewed as small (tens of eV) splittings of those levels.

Figure 6 shows the change of level density found, with excitation energy in the compound nucleus. The error bars are simply Poisson statistics based on the number of 250 eV block intervals (48). The data have also been examined with 2, 5, and 18 keV sampling intervals. The lowest three energy points are based on resonance counting[3,14,15] and the fourth from our own resolved resonance data from 2.6 to 4.8 keV. The dashed curve is a guide to the eye.

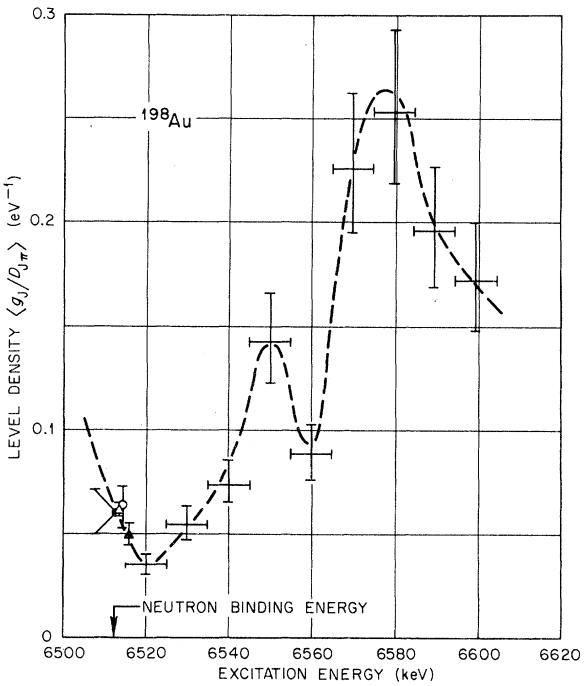

FIG. 6. The density of compound nuclear levels in ^{198}Au as a function of excitation derived from the fluctuations in the (n, γ) cross section of ^{197}Au. The open and closed circles and open triangle are from earlier work (Refs. 3, 4, 15); the closed triangle from our own 2597–4827 eV resonance analysis. The dashed curve is a guide to the eye hinting at intermediate structure peaks of width 10–20 keV and spacing ~40 keV.

V. DISCUSSION

The strength functions found to best represent the local average capture cross section to 90 keV are not unique and the data can be fitted nearly as well in a statistical sense by trading off one strength for another, to say nothing of freeing more theoretical parameters such as spin and parity dependences of the average widths. As an example, our data were fitted with a slightly lower χ^2 by weighting with the inverse square of the standard deviation of counting at each point of the curve.[16] The parameters found by the nonlinear least squares program were $S^0 = (0.93 \pm 0.13) \times 10^{-4}$, $S^1 = (0.29 \pm 0.07) \times 10^{-4}$, $S^2 = (0.57 \pm 0.18) \times 10^{-4}$, and $\Gamma_\gamma/D_0 = 0.0120 \pm 0.0017$. The standard deviations shown are entirely unrealistic as they do not take account of the strong correlations among the parameters. We believe a better set of parameters is obtained by weighting the data for energy independent fractional deviation from the fitted curve as this best represents the local average capture strength as parametrized by the four strength function model. This procedure recognizes that the statistical counting errors are unimportant compared to the nuclear resonance fluctuations. Again, the correlation makes the choice of how much to increase the computed errors for a comparison with other work a rather arbitrary matter of judgement. Our value $(1.6 \pm 0.2) \times 10^{-4}$ for S^0 compares well with the lower energy values $(1.5 \pm 0.3) \times 10^{-4}$,[14] $(2.0 \pm {}^{0.24}_{0.21}) \times 10^{-4}$,[15] and the spin weighted average $(1.6 \pm 0.5) \times 10^{-4}$.[13] Our p-wave value $(0.5 \pm 0.1) \times 10^{-4}$ applies primarily to a higher energy range, roughly 10-100 keV but is in agreement with the recent value of Carmarda[17] $(0.4 \pm {}^{0.4}_{0.3}) \times 10^{-4}$ which is determined from total cross section data primarily between 60 and 600 keV. The present result is also compatible with our earlier value $(0.3 \pm 0.3) \times 10^{-4}$,[4] but not with the Karlsruhe capture result $(0.19 \pm 0.04) \times 10^{-4}$.[18] The d-wave strength function found $(0.7 \pm 0.2) \times 10^{-4}$ is only about half the s-wave strength, contrary to the common assumption of equality,[17] and in disagreement with an earlier value $(1.4 \pm 0.4) \times 10^{-4}$.[18] Clearly the strength function values found to give acceptable fits to capture data should be used with caution. Not only do unrecognized systematic errors (in flux shape for example) have a strong influence, but the theoretical basis has been oversimplified to reduce the number of adjustable parameters. The expected change in average radiative width with parity has been mentioned as an example.[18]

TABLE II. Gold capture cross section averaged over ^{7}Li(p,n) source yield.

ΔE_p (keV)	E_n (keV) Range	Average (Ref. 4)	$\bar{\sigma}(n,\gamma)$ (mb)	$\bar{\sigma}(E_{av})$ (from Fig. 3)
0.5	23.1–36.5	29.6	576.7	584.1
1.0	20.7–39.6	29.8	570.6	581.5
1.5	18.9–42.2	30.0	570.1	578.8
2.0	17.5–44.3	30.3	570.0	576.2
2.5	16.3–46.3	30.5	570.2	573.7
3.0	15.3–48.1	30.8	570.6	571.2
3.5	14.3–49.8	31.0	571.0	568.7
4.0	13.5–51.4	31.2	571.3	566.2

Average resonance parameters have been officially requested to 2% accuracy in our energy range for use as a primary capture standard.[19] It is clear from our work that the average parameters are not adequate for this purpose; the actual structure as a function of energy can give local average cross sections departing by several percent from the over-all average calculated from the average parameters. Only in the case of the very broad neutron spectrum from the ^{7}Li(p,n) reaction close to the threshold do these departures seem acceptably small. Table II shows the average of our data over this spectrum as a function of additional broadening for the ideal case of a uniform lithium (or lithium compound) target and no proton energy spread. It is clear that for typical incident proton energies 3 keV above threshold and an energy spread of 1 keV or less, that the average is within a fraction of 1% of the strength function average. Over the whole range shown the largest difference is less than 2%. Even in the usual case where the lithium target deterioration during an experiment is unknown and the proton energy unreported the structure in the gold cross section as a function of energy can hardly introduce a 1% uncertainty.

For the 24.2 keV iron "window" flux shape (2 keV FWHM) the smooth curve of Fig. 3 gives 655 mb where a detailed integration (including the small flux asymmetry) gives 623 mb with a statistical standard deviation of 3 mb. For an antimony-beryllium 24 keV source the photon recoil energy spread is only about 160 eV but neutron scattering in the beryllium (or the sample material in the case of shell transmission) produces substantially greater energy spread and degradation in most cases. Thus it is only a reasonable guess that antimony-beryllium results for neutron activation or absorption of gold might be expected to deviate by 10% from the smooth curve of Fig. 3. An upper limit from Fig. 4 is about ±20%.

Perhaps the most comprehensive test of our absolute average values is by comparison with a recent evaluation[20] said to be in good agreement with all recent measurements. From its lower limit of 23 keV to 90 keV it deviates never more than 1½% from our strength function fit shown in Fig. 3. Above 150 keV our data, shown as a histogram, seem consistently a few percent lower than the evaluation (dashed curve) though the difference is not considered significant. From 70 keV to 550 keV, however, our data are in close agreement with recent absolute measurements.[21] A recently reported 30 keV average value, 585 ±17 mb[22] is also in satisfactory agreement with our fitted curve average (579 mb).

Finally, we need to consider the various errors inherent in our results. The data are derived from four experiments during which time six saturated 4.9 eV gold resonance calibrations were done. The calibration results agreed within their counting statistics, giving a standard deviation of the mean of 0.48%. We have since checked other gold saturated resonance calibrations against the 3.92 eV holmium and 6.7 eV uranium-238 to about ±1%.

The next most important uncertainty is the shape of the ^{6}Li(n,α) cross section (used as a flux monitor) at and above the saturated gold resonance region. We estimate its standard deviation increases with energy to about ±1% near 50 keV, ±2% near 250 keV, and perhaps ±3% near 500 keV. The energy scale is our own, but the cross sections and errors, especially near the 250 keV peak, have been reduced to agree with recent work.[23,24] The modified prescription used to calculate this cross section is given in Appendix I. In any case the derived gold cross sections can be readily corrected for further changes in the ^{6}Li(n,α) cross section as its parametrization is improved.

Statistical uncertainties in our data are 1% standard deviation (S.D.) or less for the four strength function fit or the histogram of Fig. 3. For the fluctuation data of Fig. 4 they range from well below 1% at low energy to 5% near 90 keV.[25]

The sample thickness corrections for neutrons have been discussed previously and contribute perhaps ½% uncertainty to the average cross section; less at the higher energies where the narrow p- and d-wave resonances predominate. The data were taken with a ten times thicker foil than the saturated resonance calibrations, so that the capture γ rays lost significant energy before reaching the detector. This effect has been calculated extensively for our sample and detector geometry with the gold capture γ ray spectrum.[26] A normalization uncertainty of 0.8% is attributed to residual

uncertainty in this correction. (For the individual resonances from 2.6–5 keV, this might prudently be increased to ±3%.)

The correction for direct inelastic capture γ ray detection above 250 keV mentioned earlier leads to an estimated uncertainty rising to ±1% near 550 keV.

Thus known over-all uncertainties (estimated at ±1 standard deviation and uncorrelated) are about 1.4% for the average capture cross section near 30 keV, rising to 2% (100–200 keV), 2.3% (near 250 keV), and finally to 3.3% at 550 keV.

APPENDIX I

The prescription due to Uttley for the ^{6}Li(n, α) cross section and given in the Appendix to Ref. 2 has been slightly modified to fit the more recent results.[23,24] In particular, the peak cross section near 250 keV has been reduced several percent by changing the neutron width constant of the $\frac{5}{2}^-$ state from 1.892 to 2.598. To preserve the peak position, compensatory changes in the $EL5$ formula were: 0.4311 changed to 0.49135, and 0.0372 changed to 0.0364. As indicated in Ref. 1 a further broad resonance at 2 MeV was added to improve the fit to the data from 400 to 1000 keV particularly, with its (n, α) cross section represented simply as

$$\frac{0.20}{1+X^2/E}\ \text{b}$$

with $X=(E-2)/1.5$ and E in MeV (lab).

As several laboratories are working both on improved cross section data and simultaneous parametrization of all relevant ^{6}Li$+n$ interaction data, it is hoped that our empirical parametrization can soon be superseded.

APPENDIX II

To estimate the effect of inelastic scattering followed by capture (ISC) in a thin sample such as 0.05 cm Au, we can consider the first scattering dominant. That is, we can ignore triple interactions such as elastic, inelastic, then capture. The elastic scattering followed by capture process is already evaluated as nearly 5% for 10 b scattering at the high energy limit where resonance self-protection is negligible. Inelastic scattering increases this value by drastically lowering the energy of the scattered neutron to a region where the gold capture cross section is higher. However, in the high energy limit the energy loss approaches that for elastic scattering.

Just above the first inelastic threshold [78 keV, $I=(\frac{1}{2})^+$ state reached from a $(\frac{3}{2})^+$ ground state] the inelastic cross section should be proportional to the scattered neutron's penetrability factor, here just $E_{n'}^{1/2}$. As the average gold capture cross section at low energy (say below 1 keV) should be inversely proportional to velocity, we can expect a much thinner sample with negligible resonance self-protection to show a constant ISC probability for a kilovolt or so above threshold. For the 0.05 cm sample, resonance self-protection becomes increasingly important below 1 keV so that the average ISC probability should rise from zero at threshold toward the thin sample value in the first few keV. At higher incident neutron energies, up to 100 keV or so, the inelastic cross section is still rising approximately as the penetrability but the capture cross section is falling more steeply (approximately as $E_n^{-0.68}$) and the resonance self-protection is only a few percent, thus the ISC probability decreases slowly from a few to a hundred keV above threshold. The inelastic cross section becomes measurable above this energy and shows a broad maximum (0.4 b) near 350 keV above threshold followed by a slow decrease, accentuated as other inelastic levels compete above their threshold. Extrapolating the measured cross section curve to threshold as indicated and scaling to the elastic scattering result for this sample we can see that the inelastic correction a keV or so above threshold (i.e., 79 keV E_n) is about 0.15% of the capture cross section. Where the inelastic cross section reaches its maximum, the relative correction to the capture cross section has risen to 0.25% but the correction for an equal partial cross section (0.4 b) of elastic scattering is 0.20%. Thus we make less than 0.15% error in calculating the correction as if the total scattering were elastic. Of course the second, third, and higher inelastic cross sections must also be considered as well as the decrease in elastic scattering cross section with energy, but the additional correction for the 0.05 cm sample yield due to ISC is small at all energies.

APPENDIX III

A brief summary of the average capture cross section formulas follows. Inelastic neutron scattering is assumed negligible in the range of applicability, and $l=0$, 1 dominant.

$$\overline{\sigma_{n,\gamma}} = \frac{2\pi^2}{k^2}\sum_{J^\pi}\frac{g}{D_{J^\pi}}\left(\frac{1}{\Gamma_n}+\frac{1}{\Gamma_\gamma}\right)^{-1} F(\overline{\Gamma}_\gamma/\overline{\Gamma}_n).$$

The average neutron width is gotten from a strength function as $\overline{\Gamma}_n = S_l E_n^{1/2} P_l D_{J^\pi}$. Definitions of the various terms are taken from Ref. 4 but can also be found in most standard texts.

For the case $\overline{\Gamma}_n \ll \overline{\Gamma}_\gamma$ [as for $l=2$ below 100 keV in Au(n,γ)] the summation simplifies to the as-

ymptotic form:

$$(2l+1)S_l E_n^{1/2} P_l \ .$$

The Lane and Thomas single and double neutron channel spin averaging functions (here denoted as F rather than S_v) vary little enough and slowly enough for them to be neglected in calculating the partial logarithmic derivatives.

The perturbative approach to the propagation of variance used by Egelstaff[12] is conceptually very simple. The nuclear model must be chosen to explicitly isolate the independent or uncorrelated variables if the partial derivatives alone are to suffice. These then give the change in average cross section due to given changes in each independent variable (exact in the limit of infinitesimal changes). The logarithmic derivatives do the same for fractional changes.

The propagated rates of change are then applied to the standard deviations of the theoretical distributions of the independent variables and simply squared and summed to get a relative variance estimate for the average cross section [Eq. (2)]. The term outside the bracket averages the fluctuations over a width W chosen to encompass enough individual resonances to average out the higher order terms ignored in the perturbative approach. This technique is expected to work best for nearly normal distribution functions but as indicated in the original paper works surprisingly well even for the strongly non-normal Porter-Thomas distribution with its $1/\sqrt{X}$ peak at zero (and no negative values). The other distributions (Wigner, higher index χ^2) with no poles are expected to be better behaved than the Porter-Thomas under this approach although this has not been proven.

---

*Research sponsored by the U. S. Atomic Energy Commission under contract with the Union Carbide Corporation.

[1]See B. J. Allen *et al.*, Phys. Rev. C 8, 1504 (1973) and R. L. Macklin and R. R. Winters, *ibid.* 7, 1766 (1973) for further references.

[2]R. L. Macklin, N. W. Hill, and B. J. Allen, Nucl. Instrum. Methods 96, 509 (1971).

[3]M. M. Hoffman *et al.*, in *Proceedings of the Third Conference on Neutron Cross Sections and Technology, Knoxville, Tennessee, 1971*, edited by R. L. Macklin (issued by AEC OTIE, available NTIS), CONF-710301, pp. 868–875.

[4]J. H. Gibbons *et al.*, Phys. Rev. 122, 182 (1961).

[5]R. L. Macklin, Nucl. Instrum. Methods 26, 213 (1964).

[6]D. A. Lind and R. B. Day, Ann. Phys. (N.Y.) 12, 485 (1961).

[7]E. Barnard *et al.*, Nucl. Phys. A107, 612 (1968).

[8]J. A. Nelson *et al.*, Phys. Rev. C 3, 307 (1971).

[9]Courtesy of G. de Saussure.

[10]J. J. Devaney, Nucl. Sci. Eng. 51, 272 (1973).

[11]A. Wald and A. Wolfowitz, Ann. Math. Stat. XI, No. 2 (1940); see also G. D. James, Nucl. Phys. A170, 309 (1971); and Y. Baudinet-Robinet and C. Mahaux, Phys. Rev. C 9, 723 (1974).

[12]P. A. Egelstaff, Phys. Soc. (Lond.) 71, 910 (1958).

[13]M. D. Goldberg and J. A. Harvey, in *AIP Handbook*, edited by D. E. Gray (McGraw-Hill, New York, 1972), Chap. 8f, pp. 8–218.

[14]J. S. Desjardins *et al.*, Phys. Rev. 120, 2214 (1960).

[15]R. N. Alves *et al.*, Nucl. Phys. A131, 450 (1969).

[16]As the cross sections at the low energies particularly, vary over two orders of magnitude, this gives great weight to the apparent residual cross section between resonances. The effect can be ameliorated by averaging or smearing the data in various ways, as well as by equal weighting.

[17]H. S. Camarda, Phys. Rev. C 9, 28 (1974).

[18]D. Kompe, Nucl. Phys. A133, 513 (1969).

[19]L. Stewart *et al.*, U.S. Nucl. Data Committee Report No. USNDC-6, 1973 (unpublished), and predecessors.

[20]W. P. Poenitz, AEC Symposium Series Report No. 23, August 1971 (unpublished).

[21]C. Le Rigoleur *et al.*, Centre à l'Energie Atomique Report No. CEA-N-1662, 1973 (unpublished).

[22]J. B. Czirr and M. L. Stelts, Nucl. Sci. Eng. 52, 299 (1973).

[23]W. P. Poenitz, Z. Phys. 268, 359 (1974).

[24]E. Fort and J. P. Marquette, also M. S. Coates, G. J. Hunt, and C. A. Uttley, in Proceedings of the Second IAEA Panel on Neutron Standard Reference Data, Vienna, 1972 (unpublished).

[25]Tabulated data averaged over small energy intervals and punched on computer cards have been prepared for limited distribution.

[26]We are indebted to O. A. Wasson for advice on the relevant changes in the gold capture spectrum near 24 keV vs thermal and 4.9 eV.